Forest Science and Technology

ISSN: 2158-0103 (Print) 2158-0715 (Online) Journal homepage: www.tandfonline.com/journals/tfst20

Bi-temporal ALS assessment of vertical-horizontal forest structures and their structural association in a temperate urban forest

Seunghyeon Lee, Yonghwan Kim, Dohee Kim, Hansoo Kim & Youngkeun Song

To cite this article: Seunghyeon Lee, Yonghwan Kim, Dohee Kim, Hansoo Kim & Youngkeun Song (17 Aug 2026): Bi-temporal ALS assessment of vertical-horizontal forest structures and their structural association in a temperate urban forest, Forest Science and Technology, DOI: 10.1080/21580103.2026.2712965

To link to this article: https://doi.org/10.1080/21580103.2026.2712965

FOREST SCIENCE AND TECHNOLOGY
https://doi.org/10.1080/21580103.2026.2712965

RESEARCH ARTICLE

OPEN ACCESS Check for updates

Bi-temporal ALS assessment of vertical-horizontal forest structures and their structural association in a temperate urban forest

Seunghyeon Lee[a,b], Yonghwan Kim[a], Dohee Kim[a,b], Hansoo Kim[c] and Youngkeun Song[a,b,d]

[a]Interdisciplinary Program in Landscape Architecture, Seoul National University, 1 Gwanak-ro, Gwanak-gu, Seoul 08826, Republic of Korea; [b]Integrated Major in Smart City Global Convergence, Seoul National University, 1 Gwanak-ro, Gwanak-gu, Seoul 08826, Republic of Korea; [c]Climate, Environment and Energy Research Division, Gyeonggi Research Institute, 1150 Gyeongsu-daero, Jangan-gu, Suwon 16207, Gyeonggi-do, Republic of Korea; [d]Department of Environmental Design, Graduate School of Environmental Studies, Seoul National University, 1 Gwanak-ro, Gwanak-gu, Seoul 08826, Republic of Korea

ABSTRACT

This study utilized high-density, bi-temporal airborne laser scanning (ALS) data (late-autumn and early-spring) to quantify vertical and horizontal structural features of four vegetation layers (shrub, subtree, tree, and big-tree) in urban forests of Gwacheon-si, Republic of Korea. Field validation against 1,074 polygons showed that ALS-derived subtree coverage had the lowest bias, with overestimation in the tree layer and underestimation in the shrub layer. Clear species- and season-specific patterns emerged: deciduous species such as *Castanea crenata* showed substantial canopy loss in the early-spring period, whereas evergreen species like *Pinus densiflora* remained relatively stable across seasons. Significant positive associations between ALS-derived vertical point distribution and horizontal coverage were observed, particularly in the tree and big-tree layers, and these persisted after controlling for mean canopy height (partial r = 0.75-0.98 in the big-tree layer). Structural features consistently differentiated into two functional groups - an upper canopy group (tree/big-tree) and a lower strata group (subtree/shrub) - each with distinct correlation patterns and seasonal sensitivities. By resolving these associations across species, seasons, and layers, this study demonstrates the value of bi-temporal ALS for species-specific structural assessment in temperate urban forests.

ARTICLE HISTORY
Received 27 October 2025
Revised 27 July 2026
Accepted 28 July 2026

KEYWORDS
Airborne Laser Scanning (ALS); Forest vertical layers; Vertical and horizontal structural features; Seasonal and species-specific variations; Structural association; Urban ecological map

1. Introduction

Forests, as dynamic and structurally diverse ecosystems, have long been recognized for their critical roles in supporting global biodiversity, regulating biogeochemical cycles, and providing essential ecosystem services (McNeely, 1994; Heidenreich & Seidel, 2022). Forest structure—particularly its vertical stratification and horizontal continuity—is closely related to functions such as habitat provision, light interception, photosynthetic efficiency, and the maintenance of biodiversity (Jucker et al., 2015; Lelli et al., 2019). For decades, the relationship between forest structure, function, and dynamics has been a central theme in ecological research (Latham et al., 1998; Zimble et al., 2003). With the rapid advancement of remote sensing technologies, the ability to quantify these structural relationships has significantly improved (Hui et al., 2019). Among these technologies, airborne laser scanning (ALS) has emerged as a pivotal tool due to its ability to provide high-resolution, three-dimensional structural data across expansive landscapes (Wang & Fang, 2020). ALS-based analyses now encompass canopy height models (CHMs), voxel-based vertical profiling, foliage density estimation, and stratification modeling (Hamraz et al., 2017; Caceres et al., 2019). These methods facilitate the quantification of forest structure across both vertical and horizontal axes, reflecting layers from the understory to the emergent canopy and crown dispersion patterns (Hilker et al., 2010; Sumnall et al., 2021).

Vertical structure is associated with species dominance and successional stages, while horizontal structure is essential for spatial continuity and ecological connectivity (Heiskanen et al., 2015; Sumnall et al., 2021). Vertical stratification is typically modeled using either fixed-height thresholds or adaptive, site-specific classifications. The fixed-height method pre-defines height ranges of each layer and evaluates vertical features consistently across sites. This approach facilitates integration with ecological datasets because standardized thresholds can be applied widely (Morsdorf et al., 2010; Latifi et al., 2016). In contrast, the adaptive method reflects local forest dynamics with greater flexibility but requires more complex preprocessing and is costly to reproduce (Hui et al., 2019; Hamraz et al., 2017). Meanwhile, analysis of horizontal structure using ALS has evolved to incorporate canopy cover percentage, return intensity variance, forest gaps, and foliage clumping indices

CONTACT Youngkeun Song songkoon@gmail.com Interdisciplinary Program in Landscape Architecture, Seoul National University, 1 Gwanak-ro, Gwanak-gu, Seoul 08826, Republic of Korea
Supplemental data for this article can be accessed online at https://doi.org/10.1080/21580103.2026.2712965

(Wang et al., 2023; Heiskanen et al., 2015; Choi et al., 2019; Shugart et al., 2010). These developments have broadened the perspective from simple canopy extent to spatial arrangement and heterogeneity.

However, existing research has largely treated vertical and horizontal structures as independent attributes, even though ecological processes are shaped by their interaction (Bergen et al. 2009; Culbert et al. 2013). Forest light regimes, species coexistence, and habitat heterogeneity depend not only on the presence of multiple layers but also on how those layers are spatially arranged and connected (Soto et al. 2024). Thus, a fragmented understanding of these axes limits our ability to explain forest productivity, regeneration, and biodiversity patterns (Rutten et al. 2015). Recent studies have demonstrated the ecological benefits of integrating both structural dimensions. For instance, Sverdrup-Thygeson et al. (2016) achieved higher accuracy in mapping boreal forest species distribution using combined vertical and horizontal ALS metrics. Coops et al. (2016) found improved prediction of avian richness when canopy height and cover were jointly considered. Nevertheless, such integrative approaches remain relatively rare and typically focus on a single acquisition period.

Importantly, seasonal dynamics and species-specific traits significantly influence ALS signal returns and vegetation detection. Deciduous canopies lose foliage during defoliated periods, reducing canopy density and altering both vertical distributions and horizontal coverage (Awaya & Araki, 2023; Heidenreich & Seidel, 2022). Evergreen species, by contrast, maintain relatively stable structures year-round. Integrating phenological variation and species-level differences is thus essential for a comprehensive understanding of spatial heterogeneity in forests (Yepez-Rincon et al., 2021). Despite these advances, few studies simultaneously assess both vertical and horizontal forest structure while accounting for species and phenology. Moreover, multi-temporal ALS analyses that incorporate ground-based validation remain rare (Davison et al., 2020; Wang et al., 2023). Recent methodological advances include dynamic stratification approaches that adapt layer boundaries to local forest conditions (Yun et al., 2022) and relative-height stratification schemes that define layers as fractions of maximum canopy height (Zhou & Li, 2023). In parallel, studies in urban forests have demonstrated that ALS-derived canopy complexity metrics can reliably distinguish structural types (Sharma et al., 2025), and that multi-seasonal ALS combined with hyperspectral imagery enhances species-level classification (Kim et al., 2024).

To address these gaps, our study utilizes high-density, bi-temporal ALS datasets collected on 3 November 2021 (late-autumn) and 2 April 2022 (early-spring) across forested regions of Gwacheon-si, Republic of Korea. Vegetation was stratified into four layers—shrub, subtree, tree, and big-tree—and both ALS-derived vertical point distribution and horizontal coverage were quantified for dominant species. Field survey data from 1,074 urban ecological map polygons validated ALS-derived coverage, enabling accuracy comparisons across layers and species. In addition to assessing seasonal shifts, we explicitly examine associations between vertical and horizontal features—both within the same season and across different seasons—to evaluate structural coupling and cross-season consistency. This dual-axis and dual-season framework allows us to test whether structural characteristics observed during the late-autumn period can predict those in the early-spring period, thereby assessing the cross-season consistency of ALS-derived metrics.

Accordingly, we addressed the following research questions:

1. How reliably does ALS estimate vegetation coverage across vertical layers and species compared to field observations?
2. How do ALS-derived vertical and horizontal structural features vary across species and seasons (late-autumn and early-spring) in a temperate urban forest?
3. To what extent is the vertical-horizontal association layer- and species-dependent, and robust to canopy height and spatial autocorrelation?

The existence of covariation between ALS-derived vertical and horizontal canopy metrics is itself well established (Leiterer et al., 2015; Coops et al., 2016; Wilkes et al., 2016). The novelty of this study therefore lies not in the vertical-horizontal association per se, but in decomposing it across species, season, and vegetation layer and validating it in an urban-forest setting. This species × season × layer framework provides a basis for structural modeling and management of temperate urban forests.

2. Materials and methods

2.1. Study site and materials

The study site is forested areas of Gwacheon-si, Gyeonggi Province, Republic of Korea (Figure 1). The urbanized area of Gwacheon city is centrally positioned within the city's border. The roadways to the north lead to Seoul, the capital city of the Republic of Korea, while those to the south connect to other cities in Gyeonggi Province. Large forest patches are situated on the eastern and western sides of the city.

The Gwacheon-si urban ecological map from Gyeonggi Research Institute categorizes the urban region into 10 major and 50 middle categories by land use and ecological characteristics. In total, 9,590 polygons (averagely 3,739 m^2 per each) cover the entire city region. For this research, the 4,084 polygons (averagely 5,037 m^2 per each) covering forest regions were used. The major categories for forest regions include natural forest, forest plantation, and remnant forest. Although more than 30 tree species are distributed across the forests of Gwacheon-si, we selected polygons dominated by eight main species: *Quercus mongolica, Pinus densiflora, Quercus acutissima, Robinia pseudoacacia, Pinus rigida, Castanea crenata, Quercus variabilis*, and *Pinus*

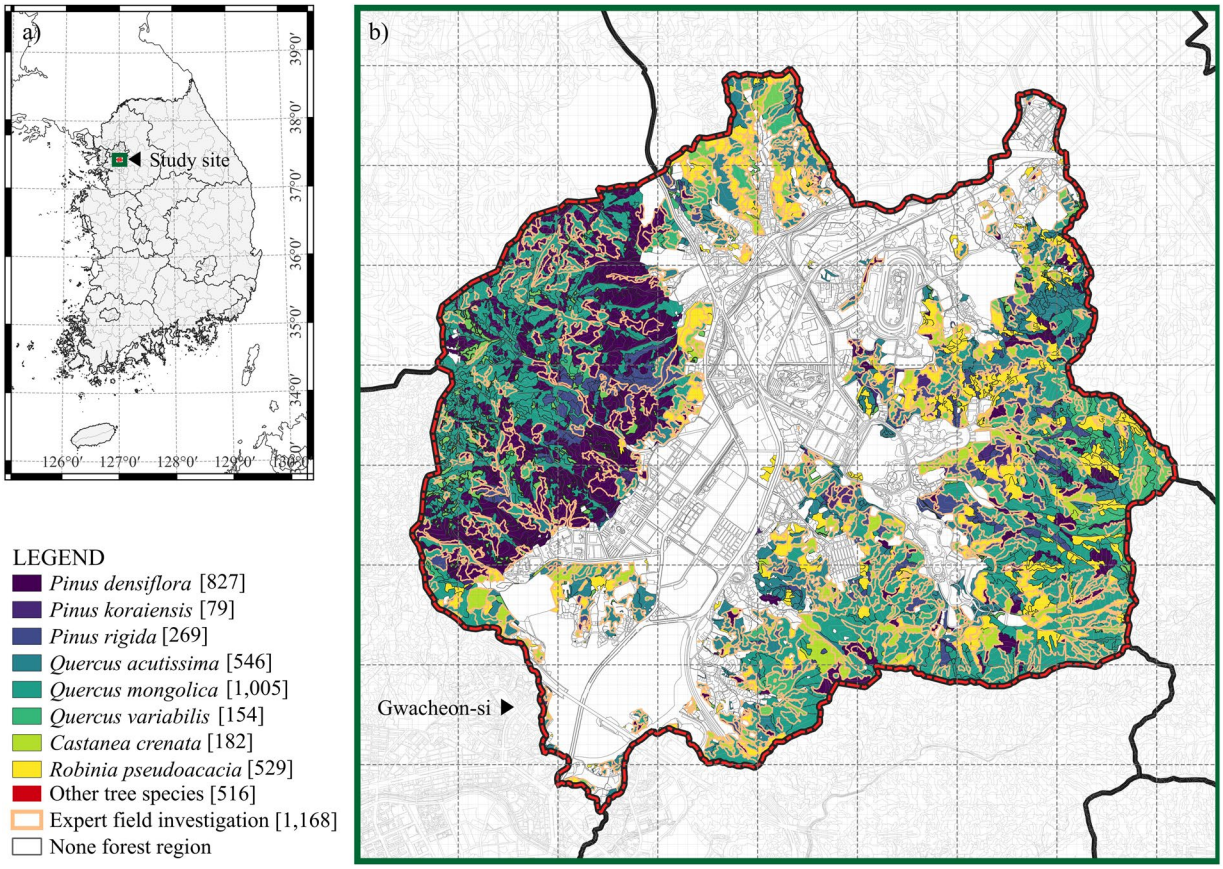

Figure 1. Location of the study site and tree species distribution; (a) study site location in the Republic of Korea; (b) distribution of eight major tree species in the study site with expert field investigation polygon borders (thick orange outlines). Numbers in brackets in the legend indicate the number of polygons.

koraiensis. Only species with more than 50 polygons were included. This yielded 3,591 polygons for the analysis.

The ALS datasets were acquired on 3 November 2021 and 2 April 2022. The 3 November acquisition corresponds to a late-autumn phenological state, when deciduous species in the study region retain foliage while approaching senescence. The 2 April acquisition corresponds to an early-spring state, prior to substantial deciduous budburst. For evergreen coniferous species (*P. densiflora, P. rigida, and P. koraiensis*), canopy structure remains relatively stable between the two periods, and the seasonal distinction primarily reflects the phenological dynamics of deciduous species. Hereafter, these two periods are referred to as the "late-autumn period" and the "early-spring period," respectively (Korpela et al., 2023; Davison et al., 2020).

The ALS data were acquired with a Leica TerrainMapper-1 sensor at a mean point density of 42.7 pts/m^2 over the forested areas; full sensor and acquisition specifications are provided in Table 1. Although reflection intensity was recorded, only the geometric distribution of returns was used in this study, as our metrics do not rely on radiometric information.

Both acquisitions were processed through an identical workflow, following the procedure described for this dataset by Kim et al. (2024), to ensure inter-period comparability. After boresight calibration (CaliGeo PRO) and ground-control-point georeferencing, orthometric heights were corrected using the Korean national geoid model (KNGeoid18). Ground returns were classified with a cloth simulation filter (CSF; Zhang et al., 2016) in R (0.1 m threshold) to generate a digital elevation model (DEM), and isolated outlier points were removed using a 0.15 m Euclidean distance threshold. Point heights were normalized to height above ground by subtracting the DEM, and artificial infrastructure within forest polygons (e.g., power transmission towers) was removed. Finally, the point cloud was voxelized at 0.5 m, with each occupied voxel counted once, so that the vertical point distribution (Eq. 1) reflects occupied voxels rather than raw return counts and is robust to local variation in point density. All structural analyses were

Table 1. Specifications of the airborne LiDAR sensor and data acquisition.

Attribute	Value
Platform	Cessna Grand Caravan 208B
Sensor model	Leica TerrainMapper-1
Date of acquisition	3 November 2021 (late-autumn); 2 April 2022 (early-spring)
Laser wavelength (nm)	1,064
Beam divergence (mrad, 1/e2)	0.25
Pulse repetition frequency (MHz)	2
Field of view (°)	20-40
Maximum number of returns	5
Scan overlap (%)	28
Flying height (ft)	6,000
Point density (pts/m^2)	42.7
Vertical accuracy (cm)	< 5 (1 SD)
Horizontal accuracy (cm)	< 13 (1 SD)
Recorded attributes	Range, intensity, GPS time, return number

performed on the normalized, voxelized point clouds clipped to the forest polygon boundaries.

2.2. Methods

Our ALS analyses quantified two structural dimensions—ALS-derived vertical point distribution and horizontal coverage—for four vegetation layers defined by fixed canopy-height thresholds: shrub (0.5–2.0 m), subtree (2.0–8.0 m), tree (8.0–16.0 m), and big-tree (16.0–30.0 m). Points below 0.5 m were excluded as ground returns and near-ground noise.

These thresholds are grounded in both established ALS stratification conventions and site-specific conditions. The 0.5 m lower bound is a widely adopted standard for separating vegetation from ground returns (Latifi et al., 2016; Wang et al., 2023). The 2.0 m boundary between the shrub and subtree layers follows the Korean National Forest Inventory (NFI) definition of shrub vegetation (<2 m) and is consistent with Morsdorf et al. (2010), who applied the same threshold in multi-layered Mediterranean forests. The 8.0 m boundary between the subtree and tree layers aligns with both Morsdorf et al. (2010), who distinguished lower canopy (<8 m) from upper canopy (≥8 m), and Hamraz et al. (2017), who demonstrated reliable ALS segmentation of understory trees below 8 m at point densities exceeding 6 pts/m^2. The 16.0 m boundary between the tree and big-tree layers reflects the canopy height distribution of the study species: the median recorded tree height across the eight dominant species in the Gwacheon urban ecological map is 12.5 m. The 30.0 m upper bound corresponds to the observed maximum canopy height across the study site.

We note that fixed-height stratification is one of two major approaches in the ALS literature. The alternative—adaptive or relative-height stratification—defines layer boundaries as proportions of local maximum canopy height (Zhou & Li, 2023). Yun et al. (2022) demonstrated that adaptive stratification heights can range from 1.59 to 20.93 m across plots, highlighting the limitations of fixed thresholds in heterogeneous forests. Seliger et al. (2023) used comparable fixed thresholds in European coniferous forests (shrub: 1–5 m, lower canopy: 5–15 m, upper canopy: >15 m). We adopted fixed thresholds because they facilitate standardized cross-species and cross-season comparisons within the study site and ensure reproducibility (Morsdorf et al., 2010).

2.2.1. ALS-derived vertical point distribution and horizontal coverage

For each polygon, the ALS-derived vertical point distribution of layer i was calculated as the ratio of voxelized ALS points within that layer to the total number of voxelized ALS points above 0.5 m (Eq. 1). The four resulting proportions sum to 1.0 and represent the relative vertical allocation of ALS returns across layers. These values are structural proxies reflecting the relative density of laser returns per layer, not direct measurements of vegetation biomass or leaf area (Wang et al., 2023; Martin et al., 2024).

$$V_i = \frac{N_i}{N_{total}} \quad \text{(Eq. 1)}$$

where N_i is the number of voxelized ALS points (0.5 m resolution) within the height range of layer i, and N_total is the total number of voxelized ALS points within the polygon above 0.5 m across all four layers.

Horizontal coverage was computed by vertically partitioning the normalized voxelized point cloud into each layer's height range and rasterizing each subset at 0.5 m resolution. The coverage for layer i was then calculated as the ratio of the total area of occupied raster cells to the total polygon area (Eq. 2).

$$H_i = \frac{C_i \times 0.25}{A_{polygon}} \quad \text{(Eq. 2)}$$

where C_i is the count of 0.5 m × 0.5 m raster cells containing at least one ALS return within the height range of layer i, 0.25 is the area of each raster cell in m^2, and A_polygon is the total polygon area in m^2.

2.2.2. Field investigation and ALS-derived vegetation coverage comparison

Traditional field investigations covered 1,168 forest polygons during the late-autumn period; of these, the 1,074 polygons dominated by the eight major tree species were used for ALS validation (Figure 1b). Basic checklists included species distributions, tree heights, crown covers, slope, and vegetation coverage proportions by vertical layers, along with additional attributes such as soil humidity, soil characteristics, litter layer height, and wildlife observations. The proportions of vegetation coverage were assessed for the shrub, subtree and tree layers. These values were compared to each of ALS-derived layer vegetation coverage proportion for the same layers.

Validation statistics including Bias (Field − ALS), Mean Absolute Error (MAE), Root Mean Square Error (RMSE), and R^2 were computed for each species × layer combination. Averages of the field investigation and ALS-derived coverage proportions were computed and compared by species. For individual polygons, the differences were calculated by subtracting the ALS results from the field investigation results. Boxplots were then drawn using the delta values, categorized by layers and species.

2.2.3. Comparison and correlation analysis of vertical and horizontal features by periods

We compared the ALS-derived vertical point distribution and horizontal coverage between the late-autumn and early-spring periods using boxplot analysis for each of the four layers. Seasonal changes were computed by subtracting early-spring values from late-autumn values. To quantify the association between vertical point distribution and horizontal coverage, Pearson correlation coefficients were computed for each combination of species, layer, and period. All

correlation coefficients are reported with 95% confidence intervals derived from Fisher z-transformation.

To assess whether the observed correlations reflect structural properties rather than artifacts of ALS measurement geometry—whereby a higher density of canopy-intercepted points mechanically reduces returns reaching lower strata—we performed partial correlation analysis controlling for mean canopy height. Mean canopy height was extracted from the original polygon-clipped LAS point clouds (prior to voxelization) for all 3,591 polygons in both periods, calculated as the arithmetic mean of all point heights above 0.5 m within each polygon. Partial correlations were computed by regressing both vertical and horizontal variables on mean canopy height and correlating the residuals. Correlation results are reported as the original correlation, its confidence interval, and the height-controlled partial correlation.

To address potential spatial autocorrelation in the correlation estimates, we computed Moran's I on the residuals of the vertical–horizontal linear relationship using a distance-based spatial weight matrix (threshold = 200 m) computed from polygon centroid coordinates. Additionally, we applied a spatial thinning algorithm with a minimum inter-polygon distance of 100 m to generate spatially thinned subsamples and re-evaluated correlations within these subsamples. The effect of polygon area on the vertical–horizontal relationship was assessed through partial correlation controlling for polygon area.

Seasonal differences in vertical point distributions were tested using the Kruskal–Wallis H test, with effect sizes reported as η^2 (eta-squared). To assess the stability of ALS-derived vertical point distributions, we performed bootstrap resampling (1,000 iterations, unweighted) for each species × layer × period combination. In each iteration, polygons were resampled with replacement and the mean vertical point proportion was computed. The 2.5th and 97.5th percentiles of the 1,000 bootstrap means defined the 95% confidence interval. The cross-season structural association (i.e., correlations between late-autumn vertical point distribution and early-spring horizontal coverage) was also evaluated using partial correlation controlling for mean canopy height, following the same residualization procedure described above.

3. Results

3.1. Validation of vegetation coverage analysis by layers

To validate the ALS-derived vegetation coverages for each vertical layer and species, we compared them with the field investigation results of 1,074 polygons dominated by eight major tree species in Gwacheon. For validation, the ALS-derived big-tree layer coverage was integrated with the tree layer coverage.

By layers, the coverage consistency differed. The ALS-derived tree layer coverage tended to be overestimated by 10 to 15 percentage points compared with field investigations, especially for broadleaf species. Across species, the subtree layer showed the highest similarity to field results, while the shrub layer showed significant underestimation by ALS (Figure 2a).

For the tree layer, ALS-based coverage estimation was more accurate for coniferous species, particularly the *Pinus* genus. The mean coverage differences (Field − ALS) of *P. densiflora, P. rigida,* and *P. koraiensis* were 1.8, −2.6, and −6.3 percentage points respectively. The other five species showed lower similarity, with larger ALS overestimations ranging from −14.2 to −7.3 percentage points. Except *P. densiflora*, ALS consistently overestimated tree-layer coverage compared with field investigation.

For the subtree layer, the absolute mean coverage differences across all species were 5.5 percentage points or less. *R. pseudoacacia* showed the smallest difference (−0.3). Broadleaf species such as *C. crenata, Q. acutissima*, and *Q. mongolica* were overestimated by more than 10 percentage points at the tree layer, but showed much smaller differences at the subtree layer (4.3, 2.9, and 1.6 respectively). With the exception of *P. densiflora,* absolute differences were consistently lower than those observed at the tree layer. Thus, the subtree layer was the least biased of the three layers, and—unlike the tree layer—did not show a systematic overestimation tendency. A low bias, however, does not necessarily indicate high reliability, because the polygon-level R^2 at this layer was only moderate (0.219).

At the shrub layer, ALS consistently underestimated coverage across species, with large differences of at least 15.6 percentage points (average across species: 23.0 percentage points). The largest discrepancies were for the *Pinus* genus: 28.4 (*P. rigida*), 27.4 (*P. densiflora*), and 24.4 (*P. koraiensis*). Even the smallest shrub-layer difference (*Q. variabilis*, 15.6) was larger than all absolute differences observed in the tree and subtree layers. The polygon-level analysis (Figure 2b) confirmed these patterns: tree-layer medians were negative across species, subtree-layer medians fell between −5.0 and 5.0, and shrub-layer medians exceeded 10 for all species.

Table 2 presents the validation statistics for each species × layer combination (n = 1,074 polygons). ALS accuracy varied systematically across vertical layers. The subtree layer showed the lowest systematic error among the three layers, with near-zero mean bias (+0.5 pp) and the smallest MAE (14.9 pp). However, its R^2 (0.219) was lower than that of the tree layer (0.377), indicating that subtree estimates are the least biased on average but explain less of the polygon-level variability in field observations. The tree layer exhibited systematic ALS overestimation (bias = −8.6 pp), which was species-dependent: coniferous species showed smaller biases (*P. densiflora*: +1.8 pp) than deciduous broadleaf species (*Q. acutissima*: −14.2 pp; *Q. mongolica*: −12.3 pp). The shrub layer showed consistent and substantial underestimation (bias = +23.4 pp), most severe under *Pinus* canopies (*P. rigida*: +28.4 pp), consistent with known ALS occlusion limitations (Sharma et al., 2025; Martin et al., 2024; Wang et al., 2023). Several broadleaf species showed very low polygon-level R^2 at the tree layer (*Q. acutissima*: 0.029; *R. pseudoacacia*: 0.038), indicating high polygon-level variability despite moderate mean bias.

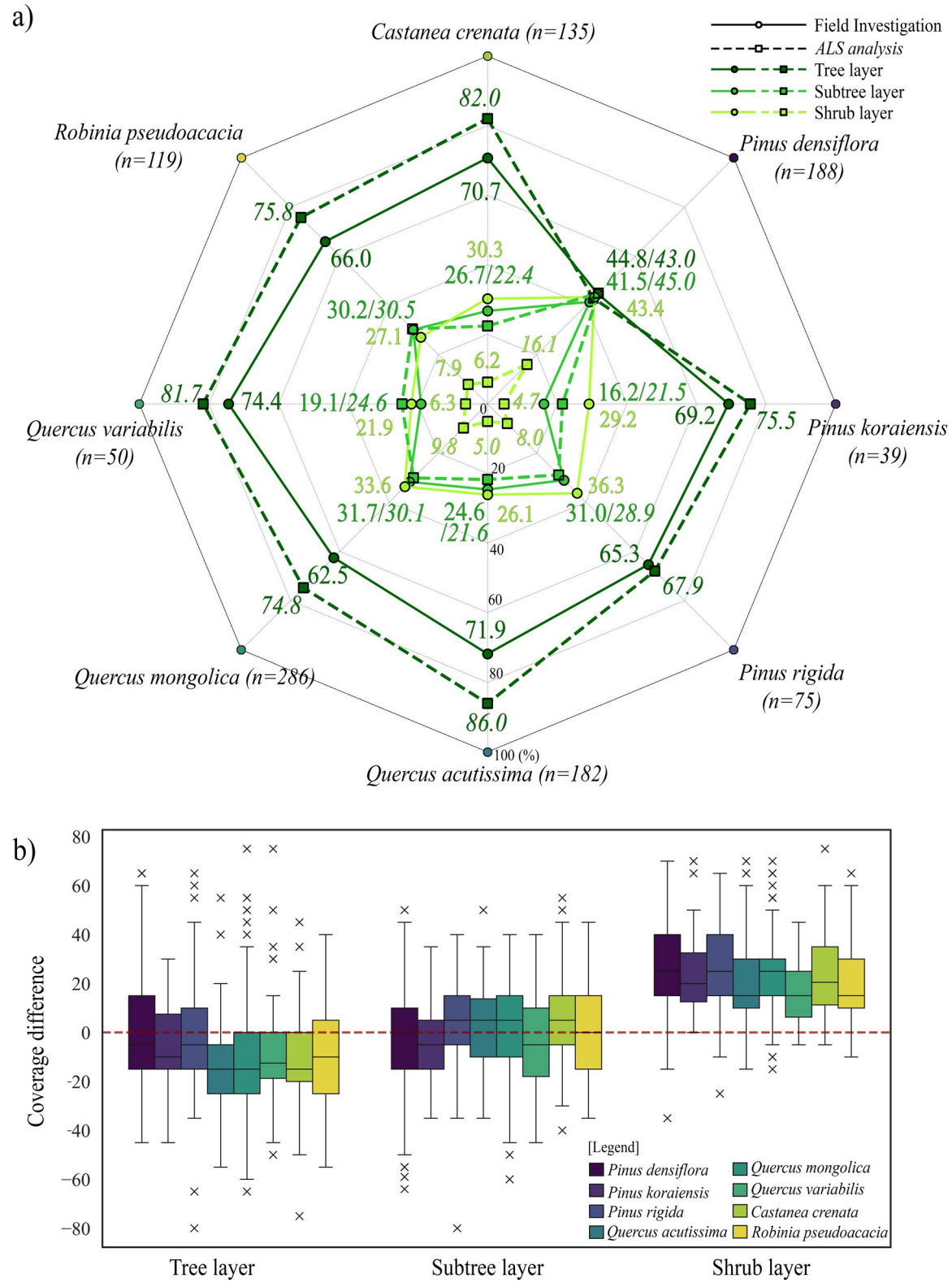

Figure 2. Comparison of field investigation and ALS-derived coverage for three layers by tree species; (a) radar chart for mean coverage comparison by species (solid line with circle: field investigation; dashed line with square markers: ALS results; dark green, green, and yellow-green lines represent tree, subtree, and shrub layer results, respectively); (b) boxplot for coverage difference (Field − ALS) of each polygon for three layers by tree species.

3.2. Vegetation vertical development and coverage analysis for bi-temporal periods

The ALS-derived vertical point distribution and horizontal coverage were analyzed across four layers (big-tree, tree, subtree, and shrub) and eight species in both the late-autumn and early-spring periods, and their differences were assessed (Figure 3).

The vertical point distribution exhibited distinct characteristics across layers and by species (Figure 3a). In the late-autumn period (Figure 3a1), the order of vertical point distributions by proportion was tree, big-tree, subtree, and shrub layer. However, for *P. densiflora*, the order was unique: subtree, tree, shrub, and big-tree layer. This result reflects the growth characteristics of *P. densiflora*, which rarely exceeds 16 m in

Table 2. Validation statistics for ALS-derived horizontal coverage against field survey data, by species and vertical layer (n = 1,074 polygons).

		Tree				Subtree				Shrub			
Species	n	Bias	MAE	RMSE	R^2	Bias	MAE	RMSE	R^2	Bias	MAE	RMSE	R^2
P. densiflora	188	+1.8	20.4	27.0	0.468	−3.5	17.3	22.8	0.295	+27.4	28.8	33.5	0.194
P. koraiensis	39	−6.3	15.8	19.1	0.309	−5.4	12.8	15.9	0.127	+24.4	24.4	29.6	0.014
P. rigida	75	−2.6	18.2	24.9	0.294	+2.1	14.3	19.3	0.300	+28.4	29.6	33.9	0.128
Q. acutissima	182	−14.2	17.4	21.1	0.029	+2.9	13.3	16.4	0.005	+21.1	21.5	27.0	0.023
Q. mongolica	286	−12.3	20.8	25.2	0.261	+1.6	15.0	18.6	0.196	+23.8	24.3	28.2	0.118
Q. variabilis	50	−7.3	18.9	24.6	0.024	−5.5	15.9	19.9	0.015	+15.6	16.4	19.9	0.043
C. crenata	135	−11.3	16.6	20.5	0.118	+4.3	13.5	17.4	0.039	+24.0	24.3	28.6	0.173
R. pseudoacacia	119	−9.8	18.1	22.9	0.038	−0.3	15.4	18.6	0.001	+19.2	19.6	24.4	0.032
All species	1074	−8.6	18.9	23.8	0.377	+0.5	14.9	19.0	0.219	+23.4	24.1	28.8	0.159

Bias = Field − ALS coverage; Bias, MAE, and RMSE are in percentage points.

height. Specifically by layers, at the big-tree layer, the three *Pinus* genus species and *Q. mongolica* showed the lowest median proportions, while the other species had values between 0.20 and 0.25. *P. densiflora* showed almost zero at the big-tree layer. At the tree layer, P. densiflora, absent in the big-tree layer, had the lowest value around 0.20, while *P. koraiensis* and *P. rigida* showed the highest values (over 0.6). At the subtree layer, *P. densiflora* showed the highest proportion (0.63), with a larger gap to other species that had less than 0.2 on average. At the shrub layer, median proportions were similar across species (below 0.05) except *P. densiflora* (0.14) and *Q. mongolica* (0.07). Notably, the *P. densiflora* shrub value is remarkably high, considering the known ALS underestimation of shrub-layer coverage (Sharma et al., 2025).

In the early-spring period (Figure 3a2), the most notable differences compared to the late-autumn period were increased proportions in the subtree and shrub layers and an intensive decrease in the big-tree layer (Figure 3a3). In the early-spring period, the tree canopy of deciduous species was largely absent, allowing laser pulses to penetrate crowns and generate more returns in lower strata (Kukenbrink et al., 2022 reported substantially higher tree detection rates under defoliated conditions). This effect was less pronounced in three evergreen species (*Pinus* genus), which showed only minor decreases in the big-tree layer, consistent with the structural stability of coniferous canopies reported by Kaminska et al. (2021).

The results of the horizontal coverage assessment (Figure 3b) were similar to the vertical point distribution analysis. Both species- and period-driven patterns exhibited similarities. However, the differences between the two periods were more pronounced for horizontal coverage. From the late-autumn to the early-spring period, the coverage of big-tree and tree layers substantially decreased. By contrast, the subtree layer experienced only minor changes (absolute median differences < 0.05 across species). The shrub layer also showed minimal change, but this result appears to be more influenced by the ALS underestimation of shrub-layer coverage than by an actual absence of seasonal change. From the combined vertical and horizontal assessment across species and seasons, horizontal coverage was more sensitive to the presence or absence of leaves than the vertical point distributions, highlighting the role of phenology (Davison et al., 2020; Korpela et al., 2023). Seasonal differences were significant across all layers (Kruskal–Wallis, $p < 0.001$), with effect sizes ranging from negligible (tree: $\eta^2 = 0.006$) to large (big-tree: $\eta^2 = 0.149$).

3.3. Structural association of vertical point distributions and horizontal coverages

Through the analysis of ALS-derived vertical point distributions and horizontal coverage across tree species and periods, we confirmed a significant structural association between the two axes (vertical and horizontal) (Figure 3). To statistically quantify these associations, we conducted a correlation analysis by species and periods for four layers. The results for each species are presented as heatmaps, with the thick black rectangles indicating same-period results (Figure 4).

For every species, during the same period and within the same layer, the vertical and horizontal features exhibited notably high correlations. With the exception of *Q. variabilis* in the early-spring period, all big-tree correlations exceeded 0.92. At the tree layer, correlations generally exceeded 0.78 across both acquisition periods, except for lower values in *R. pseudoacacia* during late-autumn and in *C. crenata* during both periods. Most subtree and shrub layer correlations were above 0.80, but they were not as high as those observed in the big-tree layer. These results indicate that the structural association between vertical and horizontal features is strongest at the uppermost vertical layer, consistent with Leiterer et al. (2015) who found that vertical layering and horizontal patchiness co-varied systematically. In addition, some species exhibited cross-season structural consistency. Among evergreen trees, *P. densiflora*'s late-autumn vertical point distribution at the tree layer correlated strongly with early-spring horizontal coverage ($r = 0.89$), and the reverse pairing was also high ($r = 0.85$). Among deciduous species, *Q. acutissima*'s late-autumn big-tree vertical feature and early-spring big-tree coverage had a correlation of 0.80.

Based on the correlation analysis, the four layers can be grouped into two functional groups: the big-tree and tree layer group, and the subtree and shrub layer group. Regardless of the acquisition period, vertical and horizontal features within the same group tend to exhibit a positive correlation, while between-group relationships primarily show a negative correlation. These trends were most evident for *P. densiflora, P. rigida*, and *Q. mongolica*, where the cross-group negative correlation reached −0.91, −0.90, and −0.90, respectively. These results indicate distinct structural

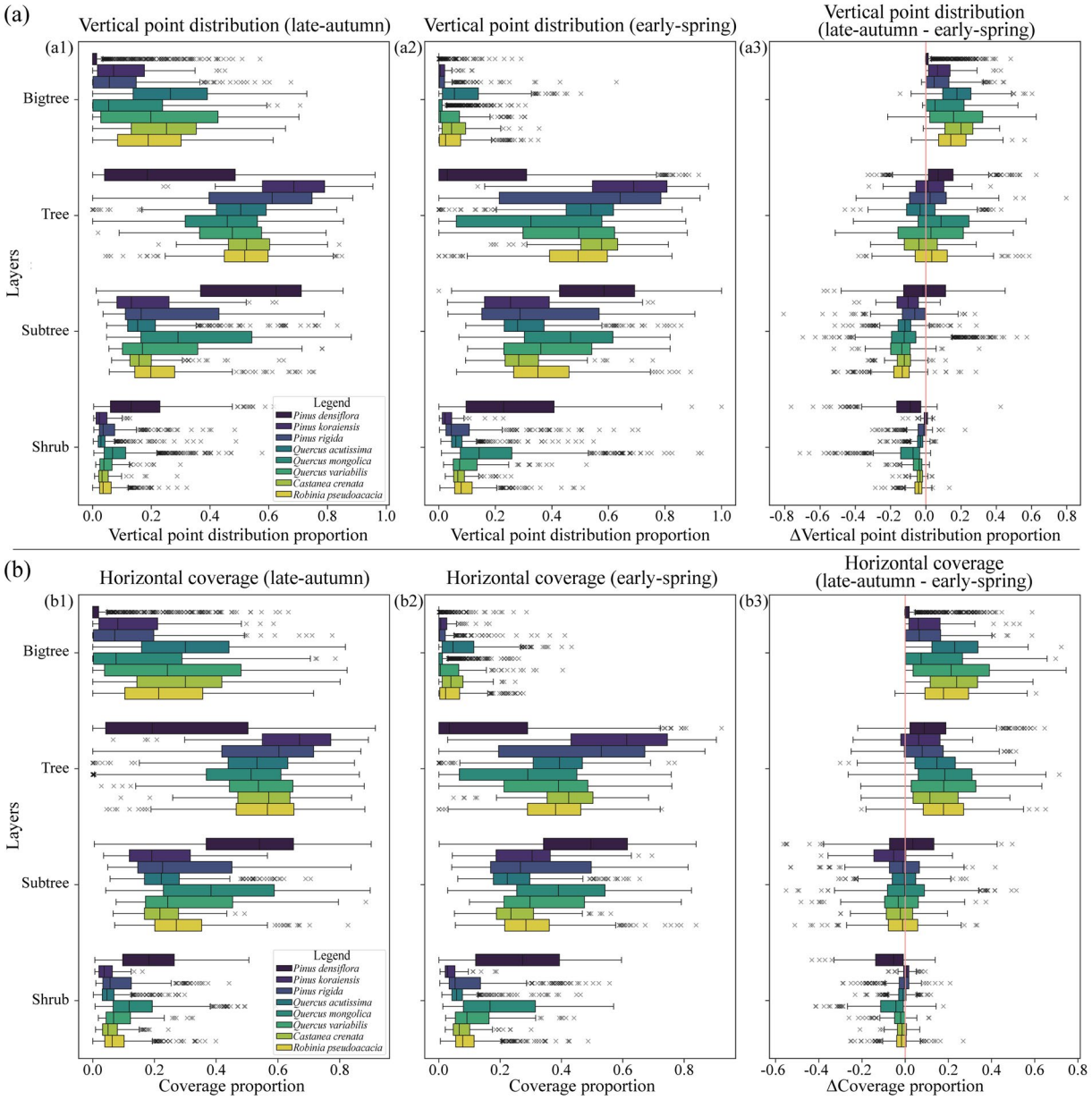

Figure 3. Assessment of ALS-derived vertical point distributions and horizontal coverage by tree species and layers across late-autumn and early-spring periods. (a) Vertical point distribution assessment: (a1) late-autumn period; (a2) early-spring period; (a3) difference (late-autumn minus early-spring). (b) Horizontal coverage assessment: (b1) late-autumn period; (b2) early-spring period; (b3) difference (late-autumn minus early-spring).

boundaries between the subtree and tree layers for certain species.

To quantify the precision of each correlation estimate, all coefficients were reported with 95% confidence intervals (Fisher z-transformation; Table 3). Confidence intervals were narrowest for species with large sample sizes and strong correlations (e.g., *P. densiflora* big-tree layer: r = 0.982 [95% CI: 0.980, 0.985], n = 827) and widest for the smallest species sample (*P. koraiensis* subtree layer: r = 0.781 [0.677, 0.855], n = 79). Results for *P. koraiensis* should therefore be interpreted with caution due to this wider uncertainty.

The vertical–horizontal correlations persisted after controlling for mean canopy height, confirming that they are not solely artifacts of ALS measurement geometry (Table 3). All partial correlations remained statistically significant, with $p < 0.001$ for all cases except *Q. variabilis* in the early-spring subtree layer (partial r = 0.241, p = 0.003). In the upper layers, height control produced moderate reductions: big-tree partial r ranged from 0.75 to 0.98, and tree partial r from 0.59 to 0.86. These reductions indicate that canopy height partially contributes to the V–H covariance, but the retained associations are too strong to attribute to artifact alone. Interestingly, in the late-autumn period, four deciduous species exhibited a suppressor effect in the tree layer, where partial correlations exceeded the originals (e.g., *C. crenata*: 0.633 → 0.693; *Q. acutissima*: 0.784 → 0.813). This pattern was exclusive to deciduous broadleaf species and absent in all *Pinus* species, suggesting that height variability within deciduous species introduces noise that obscures the underlying V–H relationship. In contrast, lower-layer associations were more sensitive to height control. The most pronounced reduction occurred in *Q. variabilis* subtree layer (early-spring: r = 0.786 → partial r = 0.241), indicating that the V–H association in lower strata is substantially mediated by canopy height

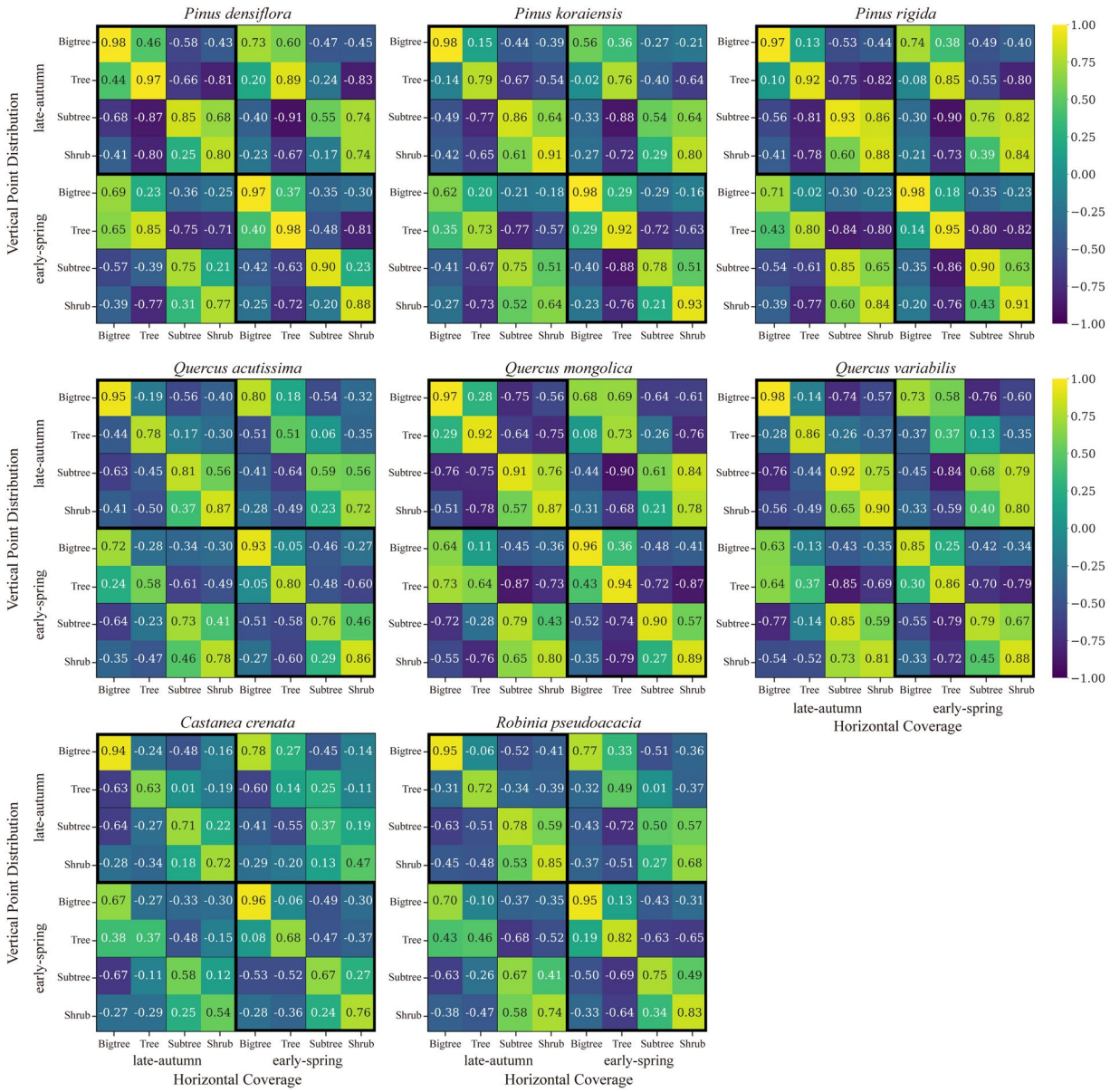

Figure 4. Correlation analysis of ALS-derived vertical point distribution and horizontal coverage by layers and periods for eight tree species. The x-axis represents horizontal coverage and the y-axis represents vertical point distribution. Thick black rectangles indicate correlations analyzed for the same period.

effects. The structural association claim is therefore strongest for the big-tree and tree layers and should be interpreted with caution for the subtree and shrub layers.

Spatial autocorrelation was present but did not inflate the reported correlations. Moran's I tests on V–H regression residuals confirmed significant positive spatial autocorrelation across most species and layers (I = 0.046–0.717; Table 4). Spatial autocorrelation was generally stronger in lower layers (shrub: mean I = 0.396; subtree: 0.322) than in upper layers (tree: 0.355; big-tree: 0.303). To test whether this spatial dependence inflated the correlation estimates, we applied spatial thinning (100 m minimum inter-polygon distance) and recomputed correlations for all layers. At the aggregate level (all species combined), correlations were virtually unchanged across all four layers: big-tree $|\Delta r|$ = 0.002, tree 0.006, subtree 0.002, shrub 0.016. At the species level, most combinations showed $|\Delta r| < 0.03$. The largest change was *C. crenata* at the shrub layer (Δr = +0.143), where thinning increased rather than decreased the correlation (r = 0.720 → 0.864). This indicates that spatially clustered *C. crenata* polygons were suppressing, not inflating, the shrub-layer association. A few other species–layer combinations showed moderate changes (*P. koraiensis* tree: +0.041; *Q. acutissima* tree: +0.032; *P. rigida* shrub: −0.033), all involving thinning-induced increases or small decreases that do not suggest inflation.

4. Discussion

4.1. Structural association between vertical and horizontal features

Our partial correlation analysis revealed that the association between ALS-derived vertical point distribution and horizontal coverage persisted after controlling for mean canopy height, with partial r values of 0.75–0.98 in the big-tree layer and 0.59–0.86 in the tree layer (all

E-ISSN 2158-0715

Table 3. Pearson correlation coefficients (r) between ALS-derived vertical point distribution and horizontal coverage, with 95% confidence intervals (Fisher z-transformation) and partial correlation coefficients (partial r) controlling for mean canopy height.

		Big-tree			Tree			Subtree			Shrub		
Species	Period	r	95% CI	partial r	r	95% CI	partial r	r	95% CI	partial r	r	95% CI	partial r
P. densiflora	Late-autumn	0.982	[0.980, 0.985]	0.960	0.970	[0.966, 0.974]	0.836	0.854	[0.834, 0.871]	0.772	0.800	[0.773, 0.823]	0.416
	Early-spring	0.969	[0.965, 0.973]	0.958	0.980	[0.977, 0.982]	0.793	0.900	[0.886, 0.912]	0.903	0.876	[0.859, 0.891]	0.538
P. koraiensis	Late-autumn	0.980	[0.969, 0.987]	0.956	0.787	[0.685, 0.859]	0.692	0.864	[0.795, 0.911]	0.588	0.911	[0.865, 0.943]	0.825
	Early-spring	0.984	[0.976, 0.990]	0.979	0.919	[0.876, 0.948]	0.606	0.781	[0.677, 0.855]	0.539	0.928	[0.889, 0.953]	0.881
P. rigida	Late-autumn	0.974	[0.967, 0.980]	0.944	0.921	[0.901, 0.937]	0.836	0.931	[0.912, 0.945]	0.708	0.876	[0.845, 0.901]	0.568
	Early-spring	0.980	[0.975, 0.985]	0.974	0.946	[0.932, 0.957]	0.730	0.900	[0.875, 0.921]	0.693	0.914	[0.892, 0.932]	0.736
Q. acutissima	Late-autumn	0.946	[0.936, 0.954]	0.783	0.784	[0.749, 0.814]	0.813	0.812	[0.781, 0.839]	0.568	0.865	[0.843, 0.885]	0.753
	Early-spring	0.926	[0.913, 0.937]	0.841	0.798	[0.765, 0.827]	0.720	0.758	[0.720, 0.792]	0.498	0.864	[0.841, 0.884]	0.742
Q. mongolica	Late-autumn	0.974	[0.971, 0.977]	0.902	0.920	[0.910, 0.929]	0.848	0.908	[0.897, 0.918]	0.531	0.867	[0.851, 0.882]	0.617
	Early-spring	0.955	[0.950, 0.961]	0.930	0.941	[0.933, 0.948]	0.585	0.901	[0.889, 0.912]	0.816	0.889	[0.876, 0.902]	0.534
Q. variabilis	Late-autumn	0.978	[0.970, 0.984]	0.863	0.856	[0.807, 0.893]	0.860	0.922	[0.894, 0.943]	0.585	0.896	[0.859, 0.923]	0.748
	Early-spring	0.851	[0.800, 0.889]	0.747	0.856	[0.807, 0.893]	0.597	0.786	[0.717, 0.840]	0.241	0.877	[0.835, 0.909]	0.664
C. crenata	Late-autumn	0.942	[0.923, 0.957]	0.797	0.633	[0.537, 0.713]	0.693	0.710	[0.630, 0.776]	0.530	0.720	[0.642, 0.784]	0.663
	Early-spring	0.959	[0.945, 0.969]	0.914	0.685	[0.599, 0.755]	0.611	0.670	[0.581, 0.743]	0.316	0.758	[0.689, 0.814]	0.646
R. pseudoacacia	Late-autumn	0.948	[0.939, 0.956]	0.816	0.715	[0.671, 0.755]	0.717	0.784	[0.749, 0.815]	0.464	0.850	[0.825, 0.872]	0.706
	Early-spring	0.945	[0.936, 0.954]	0.900	0.823	[0.793, 0.849]	0.640	0.755	[0.716, 0.789]	0.484	0.834	[0.807, 0.859]	0.646

Correlations computed for eight dominant species across four vertical layers and two acquisition periods. All Pearson correlations were significant at $p < 0.001$. All partial correlations were also significant at $p < 0.001$, except for *Q. variabilis* in the early-spring subtree layer ($p = 0.003$).

$p < 0.001$). This height-controlled association reflects canopy structure only in part. Within a layer, the vertical point distribution and the horizontal coverage are two projections (relative point count and rasterized occupancy) of the same occupied-voxel set, so a positive within-layer correlation is expected by construction even without any ecological coupling, and controlling for mean canopy height does not remove this component. The ecological interpretation therefore rests on how the association varies by species, season, and layer, which a purely constructional or geometric baseline cannot produce, rather than on the correlation magnitude itself. Nevertheless, the moderate reduction in correlation magnitudes after height control (mean reduction: $\Delta r \approx 0.08$ in the big-tree layer) suggests that a portion of the covariance is attributable to the shared influence of canopy height on both metrics, a methodological coupling that is inherent to any ALS-derived structural variable.

This dual interpretation—partly ecological, partly measurement-related—aligns with Leiterer et al. (2015), who found that voxelized ALS metrics of vertical layering and horizontal patchiness co-varied systematically across forest canopy structure types. Coops et al. (2016) similarly demonstrated that jointly considering canopy height and cover improved ecological predictions, implying a functional linkage between the two axes. In our study, the species-dependent variation in partial correlations (e.g., *P. densiflora*: 0.96 vs. *C. crenata*: 0.80 in the big-tree layer) and the systematic seasonal shifts observed only in deciduous species further support an ecological, rather than purely artifactual, interpretation: if measurement geometry were the sole driver, correlation patterns would be uniform across species and seasons.

The spatial robustness analyses reinforced this conclusion. Spatial autocorrelation was detected across all layers, with Moran's I values generally higher in lower layers (Table 4). Despite this, correlations remained stable after spatial thinning across all four layers. At the aggregate level, no layer showed $|\Delta r|$ exceeding 0.016. At the species level, most combinations showed $|\Delta r| < 0.03$. The largest change was *C. crenata* at the shrub layer ($\Delta r = +0.143$), where thinning increased the correlation from 0.720 to 0.864, indicating that spatially clustered polygons were suppressing rather than inflating the association. This is consistent with Clark et al. (2025), who found that spatial dependence affected model residuals but not the primary structural relationships in GEDI-based forest structure analysis. Wang et al. (2025) similarly reported stable structural metrics across spatially independent subsamples. Polygon area also had no detectable effect on the V–H relationship.

4.2. Layer-dependent grouping and validation implications

Our analysis revealed that the vertical and horizontal structural features consistently differentiated into two functional groups, consisting of an upper canopy group (tree and big-tree layers) and a lower strata group

Table 4. Spatial robustness of vertical–horizontal correlations (all four vegetation layers). Moran's I computed on regression residuals (200 m threshold; ** p < 0.01; *** p < 0.001; n.s., not significant).

	Big-tree		Tree		Subtree		Shrub	
Species	Moran's I	Δr	Moran's I	Δr	Moran's I	Δr	Moran's I	Δr
P. densiflora	0.046***	+0.001	0.149***	−0.008	0.369***	+0.025	0.336***	+0.005
P. koraiensis	0.188**	−0.007	0.179**	+0.041	0.123 n.s.	+0.014	0.166 n.s.	−0.020
P. rigida	0.192***	−0.002	0.295***	−0.012	0.357***	−0.009	0.562***	−0.033
Q. acutissima	0.294***	−0.014	0.369***	+0.032	0.238***	−0.002	0.331***	0.000
Q. mongolica	0.277***	0.000	0.310***	−0.003	0.393***	+0.007	0.457***	+0.014
Q. variabilis	0.555***	−0.005	0.717***	−0.007	0.370***	+0.020	0.399***	+0.033
C. crenata	0.518***	+0.002	0.466***	+0.009	0.343***	+0.039	0.505***	+0.143
R. pseudoacacia	0.357***	0.000	0.351***	−0.012	0.380***	−0.022	0.408***	−0.028
All species	0.244***	−0.002	0.271***	−0.006	0.330***	−0.002	0.362***	+0.016

Spatial thinning applied with 100 m minimum inter-polygon distance. Δr = r sub − r full. – = not computed.

(subtree and shrub layers), with positive within-group and negative between-group correlations. This grouping persisted after controlling for mean canopy height, though the partial correlation magnitudes differed. In the late-autumn period, the big-tree layer retained the strongest associations (mean partial r = 0.88), followed by the tree layer (0.79), shrub layer (0.66), and subtree layer (0.59). The reversal of the subtree–shrub ranking after height control (original: subtree > shrub; partial: shrub > subtree) suggests that the subtree-layer V–H association is more dependent on canopy height as a confounding factor than the shrub layer. This layer-dependent pattern was most pronounced for *P. densiflora, P. rigida,* and *Q. mongolica*, where the cross-group negative correlation reached r = −0.91. Wilkes et al. (2016) reported similar layer-dependent scaling of ALS-derived structural metrics, and Yun et al. (2022) demonstrated that vertical–horizontal alignment was strongest in upper canopy zones and weakened in the understory due to occlusion effects.

It should be noted that the four vertical point-distribution proportions sum to unity by construction (Eq. 1), so they constitute a compositional dataset in which an increase in one layer necessarily reduces the others. Part of the negative between-group correlation underlying the two-group structure is therefore imposed by this closed-sum constraint rather than reflecting fully independent ecological variation. Accordingly, we interpret the negative cross-group correlations as consistent with, but not by themselves proof of, the functional grouping, and we place greater interpretive weight on the within-group positive associations and on the species- and season-dependent patterns, which a closed-sum structure alone cannot produce.

The validation results (Table 2) reveal a systematic, layer-dependent pattern in ALS accuracy: the subtree layer showed the lowest bias and error, while the tree layer was systematically overestimated and the shrub layer substantially underestimated. The magnitude of shrub underestimation is comparable to findings in other ALS studies. Sharma et al. (2025) reported that ALS-derived canopy base height errors averaged 3 m in urban forests, equivalent to approximately 170% of the mean canopy base height, due to occlusion effects. Wang et al. (2023) found that understory LAI accuracy (R^2 = 0.49) was substantially lower than overstory accuracy (R^2 = 0.71). Additionally, Floyd and Anderson (1987) noted that field investigations can overestimate shrub coverage through subjective visual assessment, suggesting that the observed discrepancy reflects errors from both ALS underestimation and field overestimation.

An apparent paradox emerges for certain species: *Q. acutissima* showed the lowest field-ALS agreement at the tree layer (R^2 = 0.029) yet maintained a strong V–H association (partial r = 0.813). This suggests that the V–H structural coupling operates at a scale and mechanism distinct from field-ALS agreement. The low R^2 reflects polygon-level variability in field estimation of broadleaf coverage, whereas the V–H association captures the internal consistency of ALS-derived metrics across the vertical and horizontal axes. In other words, ALS may have poor absolute agreement with field observations for certain species, yet its internal structural metrics remain self-consistent. The very low explanatory power for these mature deciduous broadleaf species at the tree layer (R^2 = 0.024-0.038 for Q. acutissima, R. pseudoacacia, and Q. variabilis) likely reflects their open, horizontally extensive crowns, in which field-assessed crown cover and ALS-derived layer coverage respond differently to canopy gaps and overlapping crowns; high within-species variability in crown architecture and the subjectivity of visual field cover estimation (Floyd and Anderson, 1987) further attenuate the polygon-level correlation even where the mean bias is moderate.

4.3. Seasonal dynamics and species-specific patterns

Our findings show that seasonal differences in ALS-derived structural metrics were most pronounced in the big-tree layer (Kruskal–Wallis η^2 = 0.149) and least in the tree layer (η^2 = 0.006). The negligible tree-layer effect can be understood through the species-level data: *P. densiflora* and *Q. mongolica* both showed relatively large decreases in tree-layer proportions during the early-spring period (Δ = +0.091 each, i.e., higher in late-autumn), while deciduous species such as *C. crenata* (Δ = −0.024) and *Q. acutissima* (Δ = −0.021) showed slight increases in tree-layer proportions during early spring, likely due to redistribution of returns from upper to middle layers. The opposing directions of change across species result in near-zero aggregate seasonal variation, producing the negligible η^2.

At the species level, *P. densiflora* exhibited minimal seasonal change in big-tree layer proportions (Δ = +0.031), consistent with its evergreen habit and the structural stability of coniferous canopies reported by Kaminska et al. (2021). In contrast, *C. crenata* showed a substantial reduction in the big-tree layer proportion during the early-spring period (Δ = +0.187), accompanied by increased representation in the subtree and shrub layers—a pattern attributable to reduced canopy interception allowing deeper ALS penetration. Lee et al. (2026), analyzing a comparable Korean temperate mixed forest (Yangju-si) with a different analytical framework, reported maximum canopy heights of 13.5 m for P. densiflora versus 18.9 m for *C. crenata*. These values are consistent with the species-specific structural patterns observed in our study.

Notably, the increase in shrub-layer proportions during the early-spring period likely reflects a visibility bias rather than actual understory growth. The five-month interval spanning winter dormancy is insufficient for substantial woody plant growth, and the increase was disproportionately larger under deciduous canopies (*Q. mongolica*: Δshrub = −0.102) than under evergreen canopies (*P. koraiensis*: Δshrub = −0.003). This observation is consistent with Shen et al. (2024), who found that overstory canopy density directly reduced point density in understory layers, and with Kukenbrink et al. (2022), who reported substantially higher UAV-LiDAR tree detection rates under defoliated conditions (<77%) than foliated conditions (<37%).

This visibility bias also has implications for interpreting the shrub-layer V–H correlations. In most species, the shrub-layer correlation was higher during the early-spring period than during the late-autumn period (e.g., *P. densiflora*: r = 0.80 → 0.88; *P. rigida*: r = 0.88 → 0.91). Because canopy opening in early spring allows more ALS returns to reach the understory, the improved detection of existing shrub vegetation may mechanically strengthen the shrub V–H association. The early-spring shrub correlations should therefore be interpreted as reflecting both structural coupling and enhanced ALS detection capability.

4.4. Cross-season consistency

For certain species, structural metrics observed in one period were associated with the complementary axis in the other period. For example, *P. densiflora* late-autumn vertical point distribution correlated with early-spring horizontal coverage at the tree layer (r = 0.89 [95% CI: 0.87, 0.91]). However, partial correlation analysis revealed that this cross-season association is largely mediated by canopy height (partial r = 0.40), indicating that canopy height, rather than a direct structural linkage, drives much of the cross-season consistency. The degree of height-independent cross-season linkage varied substantially among species. Some deciduous species showed suppressor effects, where partial correlations exceeded the originals, suggesting that height variability obscured the underlying cross-season structural relationship.

This cross-season consistency is in line with Davison et al. (2020), who demonstrated that ALS-based structural diversity metrics performed consistently across foliated and defoliated datasets, and with Leiterer et al. (2015), who found that canopy structure types preserved their vertical and horizontal characteristics across acquisition dates. Wang et al. (2023) further reported seasonal differences in vertical LAI profile accuracy (foliated-season R^2 = 0.90 vs. defoliated-season R^2 = 0.70), suggesting that while structural patterns persist, their quantitative precision may vary by season.

4.5. Limitations and future directions

Several limitations warrant acknowledgment. First, ALS-derived vertical point distributions were not independently validated against ground-based measurements and should be interpreted as structural proxies rather than direct quantifications of vegetation density or biomass. Bootstrap resampling (1,000 iterations, unweighted) yielded narrow 95% confidence intervals for all species × layer combinations (mean CI width = 0.030; all 64 combinations had CI widths below 0.10; Supplementary Table S1), indicating stable estimates; however, the widest interval was observed for *Pinus koraiensis* (CI width up to 0.095, n = 79), reflecting the smaller sample size. Comparison with published studies supports the general reliability of ALS vertical profiles: Wang et al. (2023) validated ALS-derived vertical LAI profiles against digital hemispherical photography (R^2 > 0.80, RMSE < 0.15) and terrestrial laser scanning (R^2 = 0.97), while Martin et al. (2024) reported ALS predictions of vertical canopy fuel structure with R^2 = 0.42–0.68. Future studies should incorporate TLS or hemispherical photography for direct vertical profile validation.

Second, the vertical–horizontal correlations may partially reflect the mathematical coupling inherent to ALS point-cloud processing, whereby canopy-intercepted returns reduce the number of points reaching lower strata. This concern has been raised in other ALS studies. Wilkes et al. (2016) demonstrated that ALS-derived vertical and horizontal structures scale differently depending on canopy position. Yun et al. (2022) showed that the alignment between vertical and horizontal metrics diminishes in lower strata due to occlusion. Our partial correlation analysis mitigates but does not entirely eliminate this concern. The 0.5 m voxelization applied during preprocessing normalizes point density, partially addressing the point-density confound, but a fully independent validation would require complementary non-LiDAR data sources such as TLS or hemispherical photography.

Third, the shrub-layer underestimation (mean bias = +23.4 pp) constitutes a persistent limitation inherent to ALS technology due to canopy occlusion, as discussed in Section 4.2. Shrub-layer metrics should be interpreted with caution, particularly under dense canopy conditions.

Finally, our analysis was conducted at a single urban forest site across one seasonal cycle. Davison et al. (2020) and Leiterer et al. (2015) demonstrated structural metric consistency across seasons at individual sites, but neither extended their analysis to multiple sites or years. The generalizability of the observed structural associations to other forest types, climate zones, or inter-annual temporal scales remains to be tested through multi-site, multi-year studies. In addition, all eight species were sampled within a single urban forest under a shared climatic and management regime (Gwacheon-si); the structural associations reported here may therefore differ in rural or natural stands of the same species, where stand density, silvicultural history, and competitive context vary, and generalization will require multi-site validation spanning urban-to-natural gradients.

5. Conclusion

This study emphasizes the capability of high-density, bi-temporal ALS to simultaneously capture both vertical and horizontal structural features of urban forests, thereby revealing complex species- and season-specific variations. The novel contribution lies not in the existence of a vertical-horizontal association, which is already established in the ALS literature, but in resolving how this association - and the underlying structural metrics - vary across eight species, two phenological periods, and four vegetation layers, validated against field survey polygons in an urban forest. Validation against field surveys showed that ALS-derived coverage was least biased at the subtree layer (mean absolute difference of 5.5 percentage points or less), though with only moderate R^2, while the tree layer was systematically overestimated and the shrub layer systematically underestimated. At the tree layer, agreement was strong for coniferous species but weak for some mature deciduous broadleaf species (Q. acutissima, R. pseudoacacia, Q. variabilis), for which polygon-level coverage should be interpreted with caution. Beyond validation, the analysis revealed clear patterns of structural association. Significant positive associations between ALS-derived vertical point distribution and horizontal coverage, particularly in the tree and big-tree layers, indicate that vertical stratification and horizontal continuity are closely associated in this temperate urban forest, consistent with previously reported vertical-horizontal covariation in ALS data (Leiterer et al., 2015; Coops et al., 2016). Partial correlation analysis confirmed that these associations persisted after controlling for mean canopy height. Because the vertical and horizontal metrics are two projections of the same occupied-voxel set within a layer, part of the within-layer coupling is constructional, and the ecological signal lies in how the association varies across species, season, and layer rather than in the correlation magnitude alone. These relationships were consistent across seasons and species, and were robust to spatial autocorrelation and polygon area effects. Importantly, the vertical and horizontal structural features differentiated into two functional groups: upper canopy layers (tree and big-tree) and lower strata (subtree and shrub), each exhibiting characteristic patterns of inter-layer correlation and seasonal sensitivity. Seasonal dynamics further revealed that evergreen species, such as P. densiflora, maintained structural stability across different periods, while deciduous species, like C. crenata, exhibited substantial canopy loss and redistribution toward lower strata during the early-spring season. Cross-season correlations provided preliminary evidence of structural consistency for certain species, though partial correlation analysis revealed that much of this cross-season association is mediated by canopy height. Overall, our findings highlight the value of integrating both vertical and horizontal structural assessments to achieve a comprehensive understanding of forest spatial heterogeneity. This study also demonstrates that ALS is a valuable tool not only for species-specific structural characterization but also for capturing temporal changes in forest structure. Future studies should validate ALS-derived vertical profiles against ground-based measurements (e.g., TLS, hemispherical photography), evaluate alternative layer stratification approaches, and extend the analysis to multi-site, multi-year datasets to assess the generalizability of the observed patterns.

Acknowledgements

This work was supported by the National Research Foundation of Korea (NRF) grant funded by the Korea government (MSIT) (RS-2025-00562354). This study was also supported by the Gyeonggi Research Institute through the Gyeonggi-do Metropolitan Biotope Map Establishment Planning Study.

Conflict of interest statement

None declared.

Funding

National Research Foundation of Korea (NRF), RS-2025-00562354; Gyeonggi Research Institute.; Gyeonggi Research Institute.

Data availability statement

The airborne laser scanning and field survey datasets underlying this study contain sensitive geospatial information provided under institutional and project agreements and cannot be shared publicly. De-identified, aggregated data used for analyses may be made available from the corresponding author upon reasonable request, subject to institutional review and a data-use agreement.

References

Awaya, Y., & Araki, K. (2023). Estimating three-dimensional distribution of leaf area using airborne LiDAR in deciduous broad-leaved forest. Remote Sensing, 15(12), 3043. https://doi.org/10.3390/rs15123043

Bergen, K. M., Goetz, S. J., Dubayah, R. O., Henebry, G. M., Hunsaker, C. T., Imhoff, M. L., … & Radeloff, V. C. (2009). Remote sensing of vegetation 3-D structure for biodiversity and habitat: Review and implications for lidar and radar spaceborne missions. Journal of Geophysical Research: Biogeosciences, 114(G2). https://doi.org/10.1029/2008JG000883

Caceres, M. D., Martin-Alcon, S., Gonzalez-Olabarria, J. R., & Coll, L. (2019). A general method for the classification of forest stands using species composition and vertical and horizontal structure. Annals of Forest Science, 76(2), 40. https://doi.org/10.1007/s13595-019-0824-0

Choi, H., Song, Y., & Jang, Y. (2019). Urban forest growth and gap dynamics detected by yearly repeated airborne Light Detection and Ranging (LiDAR): A case study of Cheonan, South Korea. Remote Sensing, 11(13), 1551. https://doi.org/10.3390/rs11131551

Clark, M. L., Hakkenberg, C. R., Bailey, T. N., Burns, P., & Goetz, S. J. (2025). Changes in GEDI-based measures of forest structure after large California wildfires relative to pre-fire conditions. Remote Sensing of Environment, 323, 114718. https://doi.org/10.1016/j.rse.2025.114718

Coops, N. C., Tompaski, P., Nijland, W., Rickbeil, G. J. M., Nielsen, S. E., Bater, C. W., & Stadt, J. J. (2016). A forest structure habitat index based on airborne laser scanning data. Ecological Indicators, 67, 346–357. https://doi.org/10.1016/j.ecolind.2016.02.057

Culbert, P. D., Radeloff, V. C., Flather, C. H., Kellndorfer, J. M., Rittenhouse, C. D., & Pidgeon, A. M. (2013). The influence of vertical and horizontal habitat structure on nationwide patterns of avian biodiversity. The Auk, 130(4), 656–665. https://doi.org/10.1525/auk.2013.13007

Davison, S., Donoghue, D. N. M., & Galiatsatos, N. (2020). The effect of leaf-on and leaf-off forest canopy conditions on LiDAR derived estimations of forest structural diversity. International Journal of Applied Earth Observation and Geoinformation, 92, 102160. https://doi.org/10.1016/j.jag.2020.102160

Floyd, D. A., & Anderson, J. E. (1987). A comparison of three methods for estimating plant cover. Journal of Ecology, 75(1), 221–228. https://doi.org/10.2307/2260547

Hamraz, H., Contreras, M. A., & Zhang, J. (2017). Forest understory trees can be segmented accurately within sufficiently dense airborne laser scanning point clouds. Scientific Reports, 7(1), 6770. https://doi.org/10.1038/s41598-017-07200-0

Heidenreich, M. G., & Seidel, D. (2022). Assessing forest vitality and forest structure using 3D data: A case study from the Hainich National Park, Germany. Frontiers in Forests and Global Change, 5, 929106. https://doi.org/10.3389/ffgc.2022.929106

Heiskanen, J., Korhonen, L., Hietanen, J., & Pellikka, P. K. E. (2015). Use of airborne lidar for estimating canopy gap fraction and leaf area index of tropical montane forests. International Journal of Remote Sensing, 36(10), 2569–2583. https://doi.org/10.1080/01431161.2015.1041177

Hilker, T., van Leeuwen, M., Coops, N. C., Wulder, M. A., Newnham, G. J., Jupp, D. L., & Culvenor, D. S. (2010). Comparing canopy metrics derived from terrestrial and airborne laser scanning in a Douglas-fir dominated forest stand. Trees, 24, 819–832. https://doi.org/10.1007/s00468-010-0452-7

Hui, G., Zhang, G., Zhao, Z., & Yang, A. (2019). Methods of forest structure research: A review. Current Forestry Reports, 5(3), 142–154. https://doi.org/10.1007/s40725-019-00090-7

Jucker, T., Bouriaud, O., & Coomes, D. A. (2015). Crown plasticity enables trees to optimize canopy packing in mixed-species forests. Functional Ecology, 29(8), 1078–1086. https://doi.org/10.1111/1365-2435.12428

Kaminska, A., Lisiewicz, M., & Stereczak, K. (2021). Single tree classification using multi-temporal ALS data and CIR imagery in mixed old-growth forest in Poland. Remote Sensing, 13(24), 5101. https://doi.org/10.3390/rs13245101

Kim, D., Song, Y., Kim, H., Kwon, O., Yeon, Y. K., & Lim, T. (2024). Airborne multi-seasonal LiDAR and hyperspectral data integration for individual tree-level classification in urban green spaces at city scale. International Journal of Applied Earth Observation and Geoinformation, 136, 104319. https://doi.org/10.1016/j.jag.2024.104319

Korpela, I., et al. (2023). Influence of phenology on waveform features in deciduous and coniferous trees. Remote Sensing of Environment, 287, 113618. https://doi.org/10.1016/j.rse.2023.113618

Kukenbrink, D., et al. (2022). Benchmarking laser scanning and terrestrial photogrammetry to extract forest inventory parameters. International Journal of Applied Earth Observation and Geoinformation, 113, 102999. https://doi.org/10.1016/j.jag.2022.102999

Latham, P. A., Zuuring, H. R., & Coble, D. W. (1998). A method for quantifying vertical forest structure. Forest Ecology and Management, 104(1-3), 157–170. https://doi.org/10.1016/s0378-1127(97)00254-5

Latifi, H., Heurich, M., Hartig, F., Muller, J., Krzystek, P., Jehl, H., & Dech, S. (2016). Estimating over- and understorey canopy density of temperate mixed stands by airborne LiDAR data. Forestry: An International Journal of Forest Research, 89(1), 69–81. https://doi.org/10.1093/forestry/cpv032

Lee, S., Ha, U., Lee, H., Choe, H., Kim, H., & Song, Y. (2026). Multi-scale forest typologies using novel vertical layer metrics from airborne LiDAR in temperate mixed forests. Ecological Indicators, 185, 114798. https://doi.org/10.1016/j.ecolind.2026.114798

Leiterer, R., Furrer, R., Schaepman, M. E., & Morsdorf, F. (2015). Forest canopy-structure characterization: A data-driven approach. Forest Ecology and Management, 358, 48–61. https://doi.org/10.1016/j.foreco.2015.09.003

Lelli, C., Bruun, H. H., Chiarucci, A., Donati, D., Frascaroli, F., Fritz, O., … & Heilmann-Clausen, J. (2019). Biodiversity response to forest structure and management: Comparing species richness, conservation relevant species and functional diversity as metrics in forest conservation. Forest Ecology and Management, 432, 707–717. https://doi.org/10.1016/j.foreco.2018.09.057

Martin, M., et al. (2024). Unlocking the potential of Airborne LiDAR for direct assessment of fuel bulk density. Agricultural and Forest Meteorology, 359, 110341. https://doi.org/10.1016/j.agrformet.2024.110341

McNeely, J. A. (1994). Lessons from the past: Forests and biodiversity. Biodiversity & Conservation, 3, 3–20. https://doi.org/10.1007/BF00115329

Morsdorf, F., Marell, A., Koetz, B., Cassagne, N., Pimont, F., Rigolot, E., & Allgower, B. (2010). Discrimination of vegetation strata in a multi-layered Mediterranean forest ecosystem using height and intensity information derived from airborne laser scanning. Remote Sensing of Environment, 114(7), 1403–1415. https://doi.org/10.1016/j.rse.2010.01.023

Rutten, G., Ensslin, A., Hemp, A., & Fischer, M. (2015). Vertical and horizontal vegetation structure across natural and modified habitat types at Mount Kilimanjaro. PloS One, 10(9), e0138822. https://doi.org/10.1371/journal.pone.0138822

Seliger, A., Ammer, C., Kreft, H., & Zerbe, S. (2023). Diversification of coniferous monocultures in the last 30 years and implications for forest structure. European Journal of Forest Research, 142, 1267–1282. https://doi.org/10.1007/s10342-023-01595-4

Sharma, G., Morgenroth, J., Richards, D. R., & Ye, N. (2025). Classifying canopy complexity to assess the reliability of airborne LiDAR in urban forests. Urban Forestry & Urban Greening, 104, 129102. https://doi.org/10.1016/j.ufug.2025.129102

Shen, X., Cao, L., Ma, Y., Coops, N. C., Muise, E. R., Wang, G., & Fu, H. (2024). Estimating structure of understory bamboo for giant panda habitat by developing ALS-based methods. International Journal of Applied Earth Observation and Geoinformation, 135, 104304. https://doi.org/10.1016/j.jag.2024.104304

Shugart, H. H., Saatchi, S., & Hall, F. G. (2010). Importance of structure and its measurement in quantifying function of forest ecosystems. Journal of Geophysical Research: Biogeosciences, 115(G2). https://doi.org/10.1029/2009JG000993

Soto, D. P., Seidel, D., Hernandez-Moreno, A., Puettmann, K. J., & Donoso, P. J. (2024). Increase in forest structural complexity along a precipitation gradient is mediated by partial harvests in temperate Patagonian forests. Scientific Reports, 14(1), 13656. https://doi.org/10.1038/s41598-024-64523-5

Sumnall, M. J., Trlica, A., Carter, D. R., Cook, R. L., Schulte, M. L., Campoe, O. C., … & Thomas, V. A. (2021). Estimating the

overstory and understory vertical extents and their leaf area index in intensively managed loblolly pine plantations using airborne laser scanning. Remote Sensing of Environment, 254, 112250. https://doi.org/10.1016/j.rse.2020.112250

Sverdrup-Thygeson, A., Orka, H. O., Gobakken, T., & Naesset, E. (2016). Can airborne laser scanning assist in mapping and monitoring natural forests? Forest Ecology and Management, 369, 116–125. https://doi.org/10.1016/j.foreco.2016.03.035

Wang, Y., & Fang, H. (2020). Estimation of LAI with the LiDAR technology: A review. Remote Sensing, 12(20), 3457. https://doi.org/10.3390/rs12203457

Wang, Y., Fang, H., Zhang, Y., Li, S., Pang, Y., Ma, T., & Li, Y. (2023). Retrieval and validation of vertical LAI profile derived from airborne and spaceborne LiDAR data at a deciduous needleleaf forest site. GIScience & Remote Sensing, 60(1), 2214987. https://doi.org/10.1080/15481603.2023.2214987

Wang, Z., Singh, J., & Davies, A. B. (2025). Consistent patterns of LiDAR-derived measures of savanna vegetation complexity by season. Ecological Indicators, 170, 113061. https://doi.org/10.1016/j.ecolind.2024.113061

Wilkes, P., Jones, S. D., Suarez, L., Haywood, A., Mellor, A., Woodgate, W., … & Skidmore, A. K. (2016). Using discrete-return airborne laser scanning to quantify number of canopy strata across diverse forest types. Methods in Ecology and Evolution, 7(6), 700–712. https://doi.org/10.1111/2041-210X.12510

Yepez-Rincon, F. D., Luna-Mendoza, L., Ramirez-Serrato, N. L., Hinojosa-Corona, A., & Ferrino-Fierro, A. L. (2021). Assessing vertical structure of an endemic forest in succession using terrestrial laser scanning (TLS). Case study: Guadalupe Island. Remote Sensing of Environment, 263, 112563. https://doi.org/10.1016/j.rse.2021.112563

Yun, Z., Zheng, G., Geng, Q., Moskal, L. M., Wu, B., & Gong, P. (2022). Dynamic stratification for vertical forest structure using aerial laser scanning over multiple spatial scales. International Journal of Applied Earth Observation and Geoinformation, 114, 103040. https://doi.org/10.1016/j.jag.2022.103040

Zhang, W., Qi, J., Wan, P., Wang, H., Xie, D., Wang, X., & Yan, G. (2016). An easy-to-use airborne LiDAR data filtering method based on cloth simulation. Remote Sensing, 8(6), 501. https://doi.org/10.3390/rs8060501

Zhou, X., & Li, C. (2023). Mapping the vertical forest structure in a large subtropical region using airborne LiDAR data. Ecological Indicators, 154, 110731. https://doi.org/10.1016/j.ecolind.2023.110731

Zimble, D. A., Evans, D. L., Carlson, G. C., Parker, R. C., Grado, S. C., & Gerard, P. D. (2003). Characterizing vertical forest structure using small-footprint airborne LiDAR. Remote Sensing of Environment, 87(2-3), 171–182. https://doi.org/10.1016/s0034-4257(03)00139-1